DNS of Unsteady Flame-Wall Interaction

F. Zhang[1*], T. Zirwes[2,1], T. Häber[3], R. Wang[1], H. Bockhorn[1], D. Trimis[1], R. Suntz[3]

*feichi.zhang@kit.edu

[1]*Engler-Bunte-Institute/Division for Combustion Technology, Karlsruhe Institute of Technology, Engler-Bunte-Ring 7, 76131, Karlsruhe, Germany*
[2]*Steinbuch Centre for Computing, Karlsruhe Institute of Technology, Hermann-von-Helmholtz-Platz 1, 76344 Eggenstein-Leopoldshafen,Germany*
[3]*Institute for Chemical Technology and Polymer Chemistry, Karlsruhe Institute of Technology, Engesserstr. 20, 76131, Karlsruhe, Germany*

Abstract

Direct numerical simulations (DNS) of unsteady side-wall quenching (SWQ) of stoichiometric premixed methane/air flames operated at atmospheric condition have been conducted. Objective of the work is to study the effect of transient, relative motion between the flame and the wall on the flame-wall interaction (FWI). A W-shaped plane-jet flame is considered, which is bounded in its lateral direction by two side walls. The unsteady motion of the flame is generated by using an oscillatory wall moving in its normal direction, with a pre-defined frequency *f* and stroke length *L* (distance between min/max wall normal locations). It has been found that the time-mean quenching distance $\bar{d}_q$ and wall heat flux $\bar{\dot{q}}_w$ increase strongly with *f* and *L*. In the case of weak flow disturbances with small *f* and *L*, d_q and $\dot{q}_w$ yield a quasi-linear correlation with each other. However, a hysteresis loop for the correlation of d_q and $\dot{q}_w$ has been confirmed with increased *f* and *L*, which is attributed to the delayed response of the flame to the unsteady fluctuations of the flow and temperature fields. The behaviour of the flow-flame-wall interaction has been revealed: the unsteady flow disturbance results in a relative motion between the flame and the wall. As a consequence, d_q fluctuates in time, which leads to a different $\dot{q}_w$ or heat loss sensed by the flame. The flame adjusts its dynamics (movement) with updated $\dot{q}_w$ and the loop starts over again. The results indicate the strong impact of the unsteady flow on the FWI phenomena, which leads to delayed response of FWI to the unsteadily moving flame and modified quenching distance as well as wall heat fluxes.

Introduction

Flame-wall interaction (FWI) constitutes a common issue in engineering combustion applications, where the flame propagates against a cooled wall and is extinguished in the direct vicinity of the wall due to high heat loss. The effect of FWI contributes significantly to phenomena such as flame stabilization, burning efficiency and lifetime of the combustor. According to the essential importance of FWI, it has been studied extensively in the last decades from both viewpoints, of measurements and numerical simulations [01-17]. Dreizler and Böhm [01] and Kosaka et al. [08] performed comprehensive laser diagnostics for detailed measurements of near-wall flow and temperature fields. The same test rig has then been studied via large eddy simulations (LES) and direct numerical simulations (DNS) in 2D/3D setups and with different reaction-diffusion models in [03, 04]. Häber and Suntz [05] and Strassacker et al. [06] conducted experimental and numerical works on side-wall quenching (SWQ) of premixed methane/air flames at different equivalence ratios and have shown that the quenching distance is only weakly dependent on the wall material and heterogeneous reactions. Gruber et al. [14] studied a turbulent V-shaped hydrogen/air premixed flame anchored in a fully developed channel by means of 3D DNS, which shows a regime transition from the thin flamelet to the thickened flame regime, when the flame approaches a cold wall. Mejia et al. [07] studied the influence of wall temperatures on the flame response to acoustic perturbations, where the flame instability can be controlled or suppressed by

changing solely the temperature of the burner rim. The DNS by Poinsot et al. [09] indicates that the quenching distances and the maximum heat fluxes in a turbulent flow remain of the same order as for laminar flames and the wall acts as a sink for the flame surface density. Popp and Baum [15] presented a numerical study of FWI for a stoichiometric methane/air flame, where a single step chemical reaction failed to predict heat fluxes through the wall. Mann et al. [12] and Luo et al. [13] performed experimental and numerical studies of 1D strained laminar premixed flames impinging on a wall (head-on-quenching – HOQ), where an increase of strain rate leads to a reduced quenching distance and an increase in the wall heat flux. Zhang et al. [16] studied flame dynamics in terms of flame stretch and flame speed using 2D DNS for a SWQ setup with methane/air flames, where the Markstein number reverses its sign while the flame approaches the wall. Zhao et al. [11] performed 3D DNS of premixed turbulent combustion for a HOQ flame, where the FWI zone has been divided into an "influence zone", where the flame temperature, scalar gradient and flame dilatation start to decrease, and a "quenching zone", where chemical reactions become negligible.

Despite the progress made in the previous works, the flame extinguishes at a wall distance of the order of 0.1 mm, so that studying and modeling FWI still remains a challenging task. It is even further complicated by the transient nature of the turbulent flow, leading to scenarios of unsteady flame-turbulence-wall interaction. However, previous experimental studies and most of the numerical works of FWI have been based mostly on steady-state condition, disregarding the time history effect given by an unsteady or turbulent flow. The 3D LES/DNS of FWI with a turbulent flame have focused mainly on the statistical correlations between the chemical scalars in the FWI zone or reproducing the measured data. In addition, mostly simplified reaction mechanisms or unity Lewis number were applied in the previous 3D unsteady simulations in order to reduce computational cost.

Therefore, the objective of the present work is to reveal specifically the influence of the unsteady flow nature, which leads to a time-varying relative motion between the flame and the wall, on the FWI in a systematical and controlled manner. In order to do this, DNS with sufficiently high grid resolution, detailed reaction mechanism and transport models, as well as well-defined boundary conditions have been performed for a stoichiometric premixed methane/air flame. The unsteady flame motion has been generated by a transversally moving sidewall with prescribed oscillation frequency and amplitude, which is similar to the moving piston in an internal combustion engine. Special focus of the work is to assess the influence of the unsteady motion between the flame and the wall on the resulting quenching distance and wall heat flux, as well as their correlations in dependence upon the time and length scale of the relative unsteady motion between the flame and the wall.

Numerical Setups

DNS of a 2D side-wall quenching (SWQ) setup operated with stoichiometric premixed methane/air flames have been conducted at atmospheric condition. A rectangular domain with a length of 32 mm and width of 16 mm is used, which encloses a W–shaped flame bounded by sidewalls in the lateral direction, as shown in Fig.1. The wall temperature is set to $T_w = 293$ K. The flame is stabilized by a gas flow possessing multiple parabolic velocity profiles at the inlet, which have a velocity of 0 m/s at ¼ and ¾ of the domain width. The maximum velocity of the parabolic profiles is 1.6 m/s, which leads to a bulk flow velocity of $u_{bulk} \approx 3S_{L0}$, with the unstretched laminar burning velocity $S_{L0} = 0.32$ m/s. Burnt gas leaves the domain at the outlet of the domain, where the gradients of all flow variables are set to zero. The front and back sides of the domain have been set as symmetry planes. The unsteady motion of the flame has been created by moving the left side-wall in its normal direction with a pre-defined frequency *f* and a stroke length L (distance between min/max wall locations), whereas the right side-wall remains stationary. In this way, the entire flame is excited by the translational, oscillatory motion of the left wall, which leads to two scenarios of unsteady FWI:

- on the left hand side, the flame tip is disturbed directly by the moving wall, leading to unsteady relative motion between the flame and the wall

- on the right hand side, the flame tip is excited indirectly by the moving wall due to the periodic fluctuation of the velocity field (compression/expansion), which interacts with the stationary wall

The frequency f and the stroke range L of the oscillation have been varied in the range of $f \in [50, 100, 200]$ Hz and $L \in [1, 2]$ mm, which are selected in order to sustain the laminar flow nature. The unsteady relative motion between the flame and wall mimics the situation when a turbulent flame tip propagates against a stationary wall.

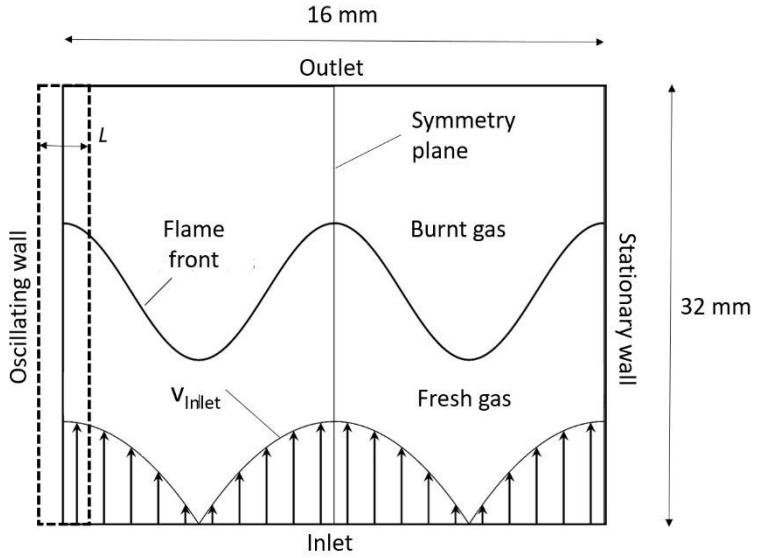

Figure 1: Schematic setup and boundary conditions used for direct numerical simulation (DNS) of unsteady side-wall quenching (SWQ).

A DNS solver developed in the framework of OpenFOAM has been used to solve the governing equations in their compressible formulations. Therewith, detailed calculations of the chemical reaction rates and transport coefficients have been applied by means of an optimized algorithm provided by Cantera [18-19]. The simulations employ a fully implicit scheme of second order (backward) for the time derivative and a fourth order interpolation scheme for the discretization of the convective term. All diffusive terms are discretized with an unbounded scheme of fourth order accuracy, too. The pressure-implicit split-operator (PISO) algorithm has been used for pressure correction. A detailed description along with validations of the DNS solver can be found in [18-21]. The chemical reactions for methane/air combustion are described by the GRI-3.0 mechanism [22] and molecular diffusion is considered by the mixture-averaged transport model. An equidistant grid length of Δ=40 µm is used, which resolves the unstretched laminar flame thickness with more than 10 cells. The simulations have been run with a time step of 0.5 µs, ensuring a maximum CFL number of 0.2.

Results

Figure.2 from left to right shows contours of the streamwise velocity u, the temperature T, the mass fraction of CH_4 and the heat release rate $\dot{q}$ calculated for the steady-state case with both lateral sides of the domain set as stationary wall. Streamlines are depicted in u–contours to illustrate the flow directions and the solid line in the T–contours indicates the flame surface identified with the isotherm T=1452 K, corresponding to the temperature at the location with the largest gradient of heat release rate from 1D unstrained flame calculations [08]. As the flame is symmetrical to its vertical axis for the steady-state case, only the left half of the flame is presented. The flow is accelerated by passing through the flame front in its normal direction, leading to bending of the streamlines at the flame surface. The flow velocity decreases to 0 at the wall due to the no-slip boundary condition, which leads to a boundary layer along the wall. The flame is extinguished by interacting with the side-wall, which can be detected from the subplots of T and q in Fig.1, which decrease to T_W and 0 while approaching the wall.

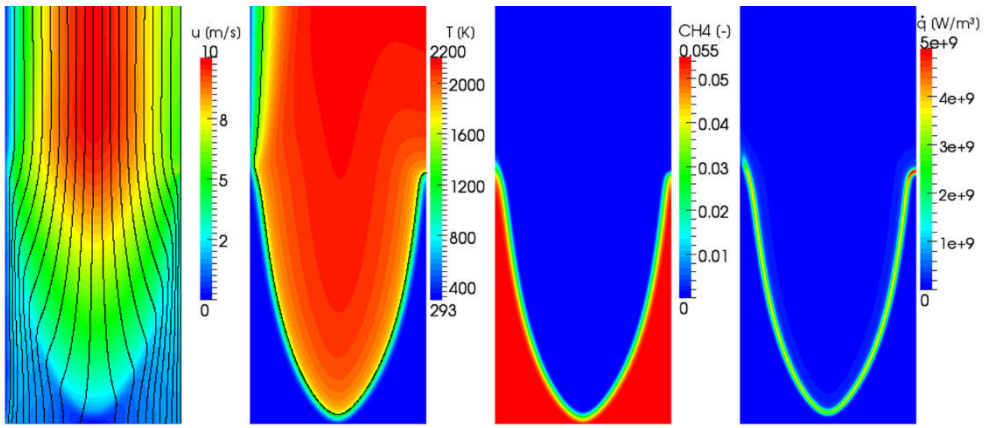

Figure 2: Contour-plots of streamwise velocity, temperature, mass fraction of CH4 and heat release rate calculated from DNS of a steady-state, stoichiometric methane/air SWQ flame.

Figure 3 illustrates contours of heat release rate for the cases with an oscillatory left wall and for a time instant corresponding to the rightmost position of the moving left wall or with the largest compression of the domain. Considering mass continuity, the flow velocity increases during compression of the domain, which leads to an increased flame length. The reversed case is given for the discharging condition. In this way, the whole flow field within the domain is excited, which interacts with the left moving wall and the right stationary wall. As the left flame part is directly disturbed by the moving wall, it is more unstable compared with the right flame branch. As indicated in the lower right plot in Fig.3, the unsteady relative motion between the flame and the wall results in fluctuation of the flame height and a variation of the quenching distance d_q on both left and right walls. Under highly unsteady conditions with high oscillation frequencies, the flame becomes even corrugated, as shown in Fig.3 for 200 Hz and 400 Hz. With further increased f and L, the flame or the flow turns to be more unstable, so that multiple flame tips interact with the walls and the current 2D assumption made for the DNS is violated. Therefore, only the cases with $f \leq 200$ Hz and $L \leq 2$ mm are considered in the following.

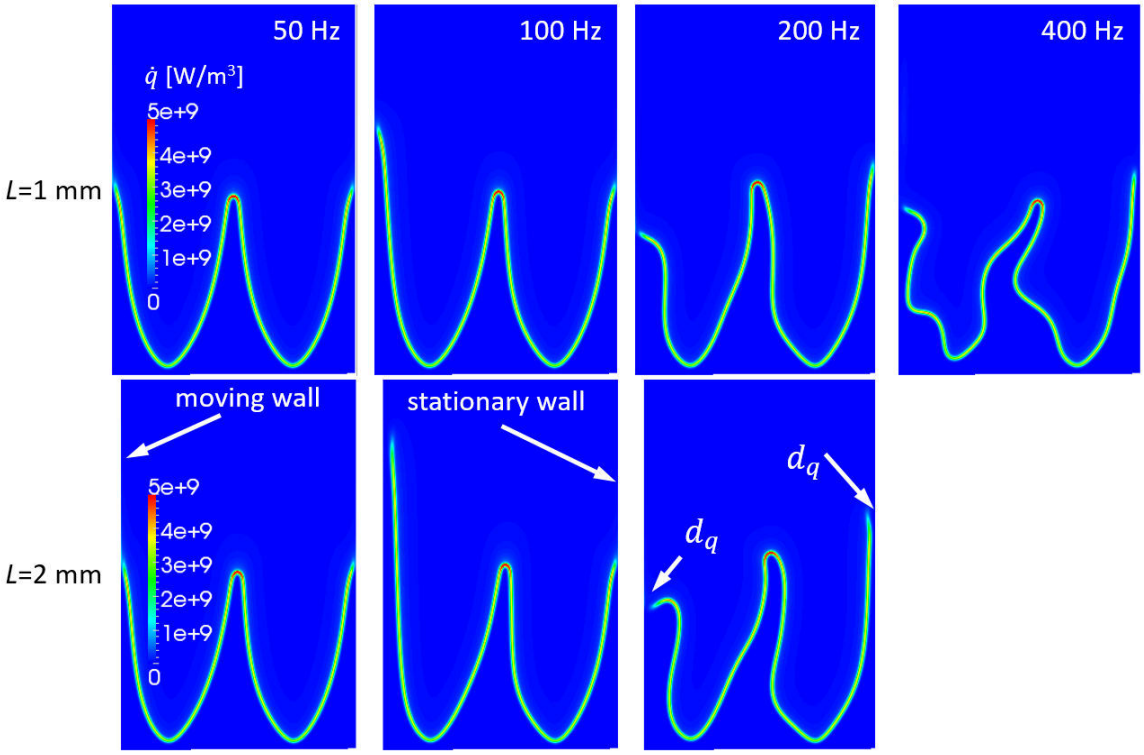

Figure 3: Instantaneous contours of heat release rate calculated from DNS of unsteady FWI for a timing corresponding to the rightmost position of the left moving wall.

Figure 4 shows temporal evolutions of the quenching distance d_q (left) and the wall heat flux $\dot{q}_w$ (right) for the left moving wall (top) and the right stationary wall (bottom), which are evaluated at the locations of the flame surface with the smallest distance to the walls. There, d_q is defined as the absolute smallest distance between the wall and the flame surface, which is always positive; $\dot{q}_w = -|\kappa \nabla T|$ points towards the wall-normal direction and is calculated directly on the wall, with κ being the thermal conductivity of the gas mixture. As the wall results in a heat loss for the flame, $\dot{q}_w$ is used here to have a negative sign. Accordingly, an increase of $\dot{q}_w$ is equivalent with a decreased magnitude of $\dot{q}_w$ or an attenuated effect of heat loss due to the wall. The dashed lines in the subplots indicate the wall distance between the instantaneous location of the moving wall and its most right position (corresponding to the most compression of the domain). The horizontal solid lines denote the steady-state solutions. The oscillatory motion of the wall leads to temporal and spatial fluctuations of the flow velocity and the temperature fields in the near-wall zone, which interact with the flame. Accordingly, d_q and $\dot{q}_w$ increase strongly with f and L compared with the steady-state solutions. Moreover, the time evolutions of d_q and $\dot{q}_w$ yield an increased phase shift with f and L (compare their maxima of the variables). The impact of the phase shift on FWI will be discussed later in more detail (see Fig.7).

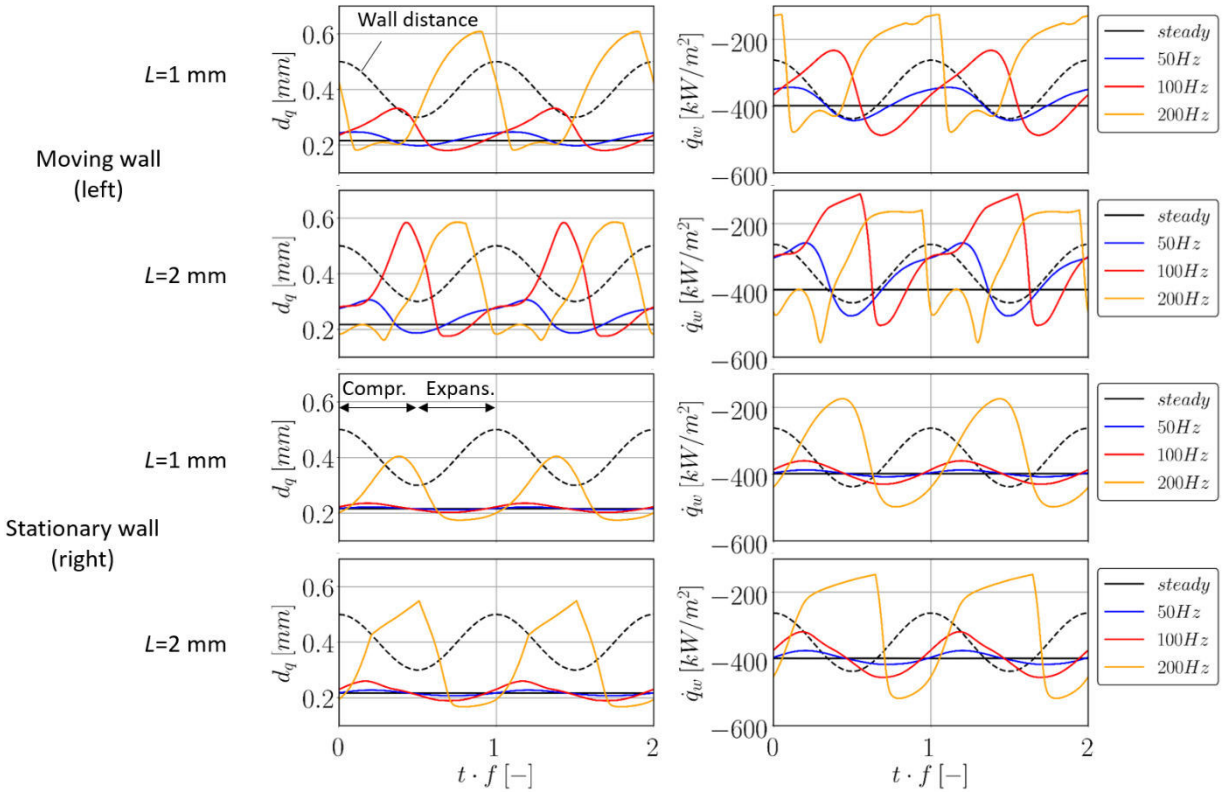

Figure 4: Time development of quenching distance (left) and wall heat flux (right) during unsteady FWI: at the top for the left moving wall and at the bottom for the right stationary wall.

Figure 5 reveals the impact of the relative motion between the wall and the flame on the time-averaged values of d_q for the left and right walls, where the horizontal solid line denotes the steady-state solution $d_{q,0}$. In accordance with the time developments of d_q shown in Fig.4, the time-mean quenching distance $\bar{d}_q$ increases with f and L for unsteady FWI. The main reason is attributed to the fact that the flame position is unbounded when the wall moves away from it, whereas its position is bounded by the wall surface when the wall moves towards the flame. As shown in Fig.4 on the left, the minimum value of d_q is only slightly smaller than $d_{q,0}$, whereas the maximum value of d_q reaches approx. 3 times of $d_{q,0}$. Although not shown here, the time mean wall heat flux $\bar{\dot{q}}_w$ increase or is less negative with an increased $\bar{d}_q$, because the temperature gradient is weakened with increased $\bar{d}_q$. In summary, it can be stated that the unsteady relative motion between the wall and the flame leads to a

considerably increased quenching distance and wall heat flux; the effect becomes stronger with increasing length scale and decreasing time scale of the relative motion. In the current work, only the smallest distance between the wall and the selected iso-surface (for the flame surface) is tracked to determine d_q. For $f = 200$ Hz and $L = 2$ mm, the flame becomes unstable or it is corrugated, so that multiple FWI zones exist on the same wall (see Fig.3). Therefore, $\bar{d}_q$ decreases at $f = 200$ Hz with increased L.

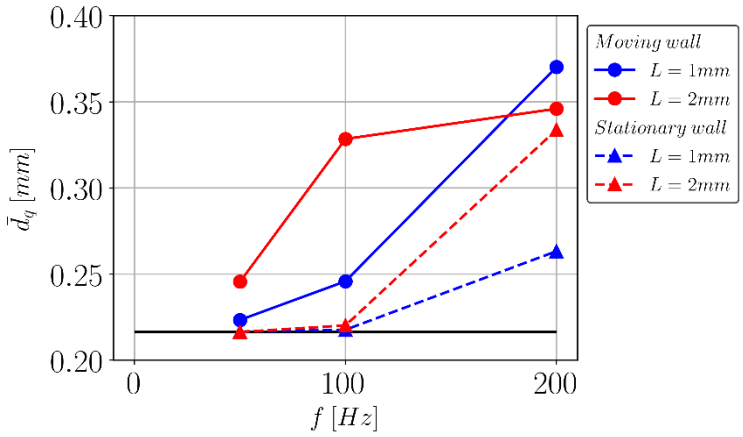

Figure 5: Time-averaged quenching distance for the left moving (left) and the right stationary wall heat flux (right) calculated from DNS of unsteady FWI.

Figure 6 shows correlations of the instantaneous quenching distance d_q with the wall heat flux $\dot{q}_w$ for the moving wall on the left and for the stationary wall on the right: at the top for L=1 mm and at the bottom for L=2 mm. The black arrows indicate the time evolution of the oscillation process which turns in counter clockwise direction. The solid circles indicate time mean values of d_q and $\dot{q}_w$. The blue arrows indicates an increased effect of unsteady FWI on the correlation between d_q and $\dot{q}_w$, which leads to an enhanced scattering of the data.

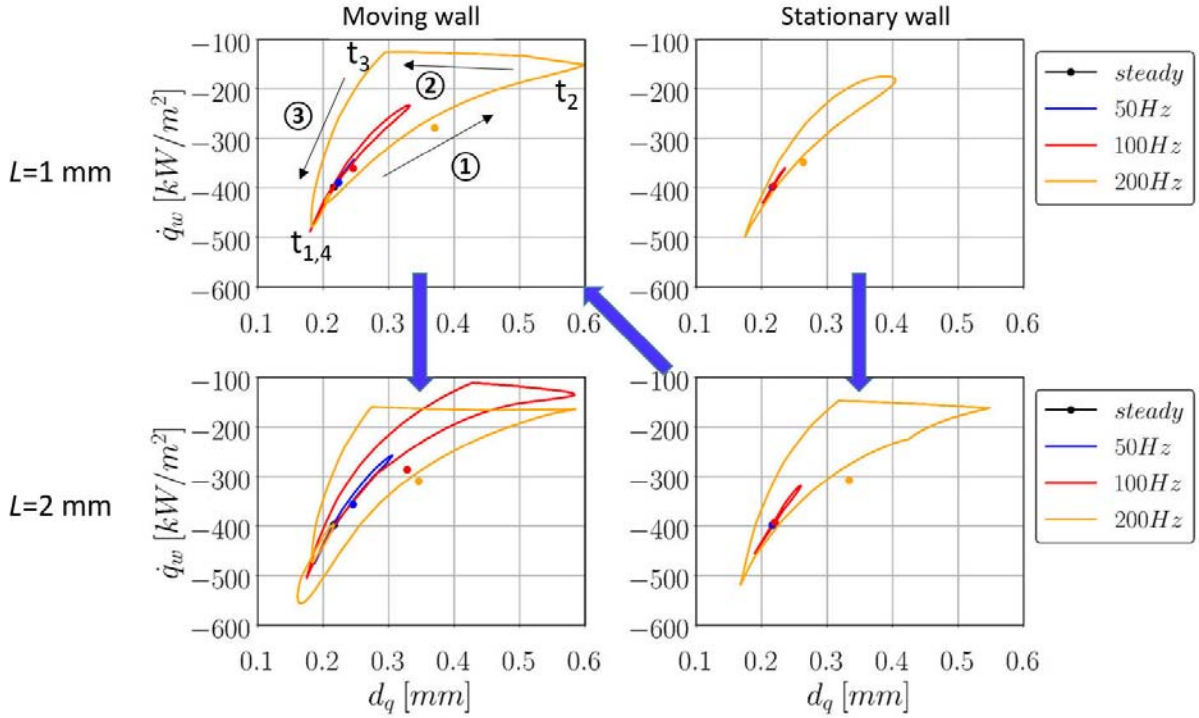

Figure 6: Correlations of instantaneous quenching distance d_q with wall heat flux $\dot{q}_w$ during unsteady flame-wall interactions.

In general, d_q and $\dot{q}_w$ yield a positive correlation, because the wall-normal gradient of temperature decreases with increased d_q: $d_q \downarrow \Rightarrow |\nabla T|_w \uparrow \Rightarrow \dot{q}_w \propto -|\nabla T|_w \downarrow$. In addition, d_q and $\dot{q}_w$ reveal a strong or quasi-linear correlation in case of small unsteady disturbances, i.e., for small *f* and *L* as well as the right stationary wall. However, a hysteresis loop with increased scattering of the correlation between d_q and $\dot{q}_w$ can be observed in the cases with large *f* and *L*. In particular, $\dot{q}_w$ increases with d_q in a disproportionate way, when the flame and the wall move relatively apart from each other, as indicated in Fig.6 by the arrow ①. Shortly after d_q has reached its maximum value and when the flame and wall turn to move relatively towards each other, d_q abruptly decreases at an almost constant $\dot{q}_w$ (indicated in Fig.6 by the arrow ②). Thereafter, the flame and the wall move relatively towards each other with a rapid decrease of $\dot{q}_w$, as indicated in Fig.6 by the arrow ③. The correlation of d_q with $\dot{q}_w$ is stronger in the range of small d_q compared with the range of large d_q, because the flame yields a more limited freedom in the range of smaller d_q.

The overall process in case of the highly unsteady FWI, i.e., in case of formation of the hysteresis loop for d_q and $\dot{q}_w$, is illustrated in Fig.7, with the subplots ① to ③ corresponding to the scenarios indicated by the numbered arrows in Fig.6. In addition, t_1 to t_4 indicate the time instants shown in Fig.6. The heat loss is weakened with increased d_q while the flame is pushed away from the wall by the flow (① in Fig.6 and Fig.7). As soon as the flame reaches the maximum flame-wall distance and turns to move back towards the wall, the flame-wall distance starts to decrease and the heat loss in terms of $\dot{q}_w$ remains approx. constant (② in Fig.6 and Fig.7). This is attributed to the retroactive (inertia) effect that the flame requires a relaxation time to adapt to the sudden change of temperature. With further decreased flame-wall distance, the heat loss decreases drastically (③ in Fig.6 and Fig.7).

Note that $\dot{q}_w$ is defined as negative in this work with $\dot{q}_w = -|\kappa \nabla T|$, considering that the wall represents a heat loss sensed by the flame (heat sink). Therefore, the smaller is d_q, the more negative or the smaller is $\dot{q}_w$. The correlation between d_q and $\dot{q}_w$ reverses its sign from positive to negative, if the magnitude of $\dot{q}_w$ is used, because $|\dot{q}_w|$ increases with d_q.

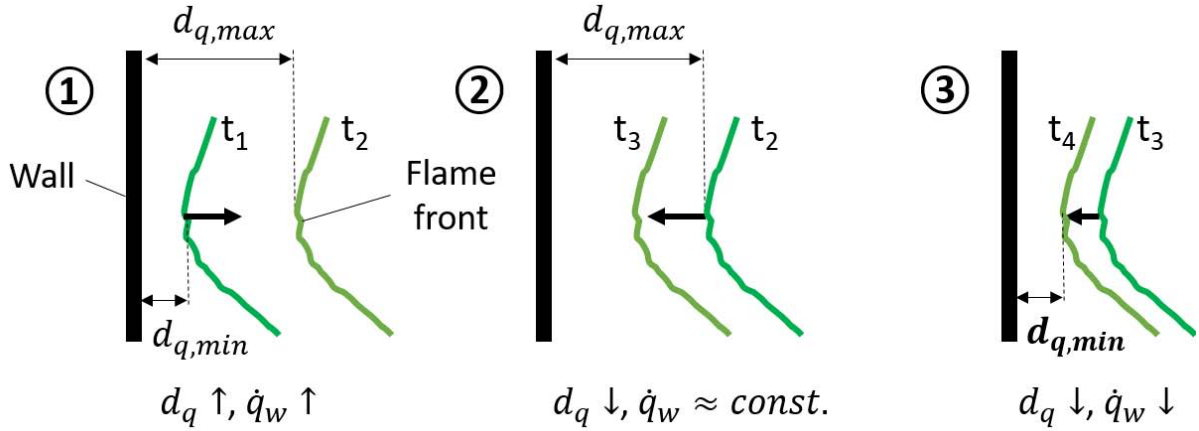

Figure 7: Illustration of the effect of highly unsteady flame-wall interaction on the correlation between wall distance and wall heat flux.

In fact, the unsteady FWI is governed by strongly time-varying flow and temperature fields in the near-wall zone. When the relative velocity between the flame and the wall is small, for instance in case of small *f* and *L*, the flame is able to follow promptly the fluctuating flow field. Accordingly, the time developments of d_q and $\dot{q}_w$ shown in Fig.4 yield only small phase shifts with each other and a quasi-linear correlation is found for d_q and $\dot{q}_w$ in Fig.6. In highly unsteady cases, however, the response of the flame to the transient changes of flow and temperature is attenuated. The transient flow stretch causes modified dynamics or moving velocity of the flame, which has a direct impact on the flame-wall distance d_q and leads to a significant variation of temperature from the unburnt to burnt state or vice

versa in the FWI zone. The apparent heat loss sensed by the flame yields a time delay with respect to the rapid change of local temperature caused by varying d_q, which results in a phase shift between the time developments of d_q and $\dot{q}_w$, as shown in Fig.4 for large f and L. This leads to the hysteresis loop for the correlations between d_q and $\dot{q}_w$, as shown in Fig.6. The behaviour of heat loss or $\dot{q}_w$ in dependence upon unsteady relative flame-wall motion is similar to that reported attenuated flame response to unsteady flow stretch with decreased time scales in [23, 24], where DNS of oscillatory premixed H_2/air flames have been performed at different excitation frequencies.

The overall behavior of the triple interaction between flow, flame and wall is illustrated in Fig.8, where the properties of the flow are represented by the turnover frequency f and the length scale L, that of the flame dynamics by the displacement and the consumption speed S_D and S_C. There, S_D represents a measure of the moving velocity of the flame and S_C the consumption rate of fuel or heat release rate. The no-slip wall with a fixed temperature T_W is regarded as passive, meaning that it is not affected by the flame. As an initial step, the flame perceives disturbances of the flow with a certain time and length scale, which affects local flame dynamics and forces the flame to move towards or apart from the wall (flame-flow interaction). Accordingly, the distance between the flame and the wall varies over time, which results in a modified wall heat flux. The flame undergoes an updated heat loss from the wall and adapts its dynamics in terms of S_D and S_C, forming a closed cycle regarding the unsteady flame-wall interaction (see Fig.8). The flow is additionally influenced by the wall due to no-slip condition (flow-wall interaction) and by the flame too, which results in an acceleration of the flow through thermal expansion with jumps of temperature, density, velocity and viscosity at the flame front. Note that a certain relaxation time is required for the flame to respond to the unsteady changes in flow stretch and temperature gradient, as discussed before.

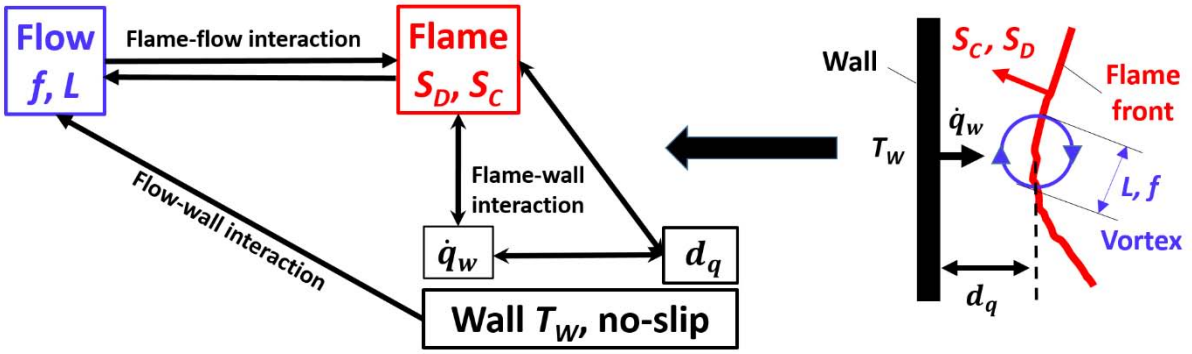

Figure 8: Illustration of fundamental principle of unsteady flow-flame-wall interactions.

Conclusion

Direct numerical simulations (DNS) have been conducted to study the effect of unsteady relative motion between the flame and the wall on the flame-wall interaction (FWI). A generic setup with a spatially oscillating wall at prescribed frequency f and stroke length L has been used to generate unsteady FWI scenarios. It has been found that the time-mean quenching distance d_q increases strongly with f and L. The reason is that the flame has more freedom for moving away from the wall compared with towards the wall. In addition, it has been found that the wall heat flux $\dot{q}_w$ yields a quasi-linear increase with d_q for the cases with small f and L. However, scattering of the correlation between $\dot{q}_w$ and d_q has been found for increased f and L, which is attributed to the delayed response of the flame to the highly-unsteady temperature gradient. The same behavior has been confirmed from the time evolutions of d_q and $\vec{\dot{q}}_w$, which yield phase shifts in cases of large f and L.

In summary, it can be stated that, in addition to the general thermo-physical parameters of the premixed fuel/oxidizer mixture, the FWI phenomenon is strongly dependent upon the unsteady flow nature, which leads to relative motion between the flame and the wall. The larger the length scale and the smaller the turnover period of the flow disturbances, the larger is the time-averaged quenching distance and the smaller is the heat loss (in magnitude). It should be noted that the effect of the

transversal motion of the flame in wall-normal direction dominates that of the flame motion in wall-parallel direction. The current work is focused on methane/air flames at stoichiometric condition and a fixed wall temperature of 293 K. Future works with extended operating parameters are necessary to justify the general validity of the obtained results in this work.

Acknowledgments
The authors gratefully acknowledge the financial support by the Helmholtz Association of German Research Centers (HGF), within the research field MTET (Materials and Technologies for the Energy Transition), subtopic "Anthropogenic Carbon Cycle" (38.05.01) and the German Research Foundation (DFG), grant number 237267381 – TRR 150. This work utilized computing resources provided by the High Performance Computing Center Stuttgart (HLRS) at the University of Stuttgart and the Steinbuch Centre for Computing (SCC) at the Karlsruhe Institute of Technology.

References
[01] A. Dreizler, B. Böhm: Advanced laser diagnostics for an improved understanding of premixed flame-wall interactions. P Comubst Inst 35 (1), 37–64, 2015.
[02] C. Jainski, M. Rißmann, B. Böhm, J. Janicka, A. Dreizler: Sidewall quenching of atmospheric laminar premixed flames studied by laser-based diagnostics. Combust Flame 183, 271–282, 2017.
[03] A. Heinrich, S. Ganter, G. Kuenne, C. Jainski, A. Dreizler, J. Janicka: 3D numerical simulation of a laminar experimental SWQ burner with tabulated chemistry. Flow Turbul. Combust 100 (2), 535–559, 2018.
[04] S. Ganter, A. Heinrich, T. Meier, G. Kuenne, C. Jainski, M. C. Rißmann, A. Dreizler, J. Janicka: Numerical analysis of laminar methane–air side-wall-quenching. Combust Flame 186, 299–310, 2017.
[05] T. Häber, R. Suntz: Effect of different wall materials and thermal-barrier coatings on the flame-wall interaction of laminar premixed methane and propane flames. Int J Heat Fluid FL 69, 95–105, 2018.
[06] C. Strassacker, V. Bykov, U. Maas: Redim reduced modeling of quenching at a cold wall including heterogeneous wall reactions. Int J Heat Fluid FL 69,185–193, 2018.
[07] D. Mejia, L. Selle, R. Bazile, T. Poinsot, Wall-temperature effects on flame response to acoustic Oscillations. P Combust Inst 35 (3), 3201–3208, 2015.
[08] H. Kosaka, F. Zentgraf, A. Scholtissek, L. Bischoff, T. Häber, R. Suntz, B. Albert, C. Hasse, A. Dreizler, Wall heat fluxes and co formation/oxidation during laminar and turbulent side-wall quenching of methane and dme flames. Int J Heat Fluid FL 70,181–192, 2018.
[09] T. Poinsot, D. C. Haworth, G. Bruneaux: Direct simulation and modeling of flame-wall interaction for premixed turbulent combustion. Combust Flame 95 (1-2) 118–132, 1993.
[10] M. Saffman: Parametric studies of a side wall quench layer. Combust. Flame 55(2), 141–159, 1984.
[11] P. Zhao, L. Wang, N. Chakraborty: Analysis of the flame-wall interaction in premixed turbulent combustion. J. Fluid Mech. 848, 193-218, 2018.
[12] M. Mann, C. Jainski, M. Euler, B. Böhm, A. Dreizler: Transient flame-wall interactions: experimental analysis using spectroscopic temperature and CO concentration measurements. Combust. Flame 161 (9), 2371–2386, 2014.
[13] Y. Luo, C. Strassacker, X. Wen, Z. Sun, U. Maas, C. Hasse: Strain Rate Effects on Head-on Quenching of Laminar Premixed Methane-air flames. Flow Turbul. Combust. 106, 631–647, 2021.
[14] A. Gruber, R. Sankaran, E. Hawkes, J. Chen: Turbulent flame–wall interaction: a direct numerical simulation study. J. Fluid Mech. 658, 5–32, 2010.
[15] P. Popp, M. Baum: Analysis of wall heat fluxes, reaction mechanisms, and unburnt hydrocarbons during the head-on quenching of a laminar methane flame. Combust Flame 108 (3), 327–348, 1997.
[16] F. Zhang, T. Zirwes, T. Häber, H. Bockhorn, D. Trimis, R. Suntz: Near Wall Dynamics of Premixed Flames. Proc. Combust. Inst. 38(2), 1955-1964, 2021.
[17] T. Zirwes, T. Häber, F. Zhang, H. Kosaka, A. Dreizler, M. Steinhausen, C. Hasse, A. Stagni, D. Trimis, R. Suntz, H. Bockhorn: Numerical Study of Quenching Distances for Side-wall Quenching Using Detailed Diffusion and Chemistry. Flow Turbul. Combust 106, 649-679, 2021.
[18] F. Zhang, H. Bonart, T. Zirwes, P. Habisreuther, H. Bockhorn, N. Zarzalis: Direct numerical simulation of chemically reacting flows with the public domain code OpenFOAM. in: High Performance Computing in Science and Engineering'14, Springer, 221–236, 2015.
[19] T. Zirwes, F. Zhang, J. A. Denev, P. Habisreuther, H. Bockhorn: Automated code generation for maximizing performance of detailed chemistry calculations in OpenFOAM. in: High Performance Computing in Science and Engineering'17, Springer, 189–204, 2018.

[20] T. Zirwes, F. Zhang, P. Habisreuther, M. Hansinger, H. Bockhorn, M. Pfitzner, D. Trimis. Quasi-DNS Dataset of a Piloted Flame with Inhomogeneous Inlet Conditions. Flow Turbul. Combust 104, 997–1027, 2019.
[21] T. Zirwes, F. Zhang, J. A. Denev, P. Habisreuther, H. Bockhorn, D. Trimis: Improved Vectorization for efficient chemistry computations in OpenFOAM for large scale combustion simulations. in: High Performance Computing in Science and Engineering'18, Springer, 2019, pp. 209–224.
[22] G. P. Smith, D. Golden, M. Frenklach, N. Moriarty, B. Eiteneer, M. Goldenberg, C. Bowman, R. Hanson, S. Song, W. Gardiner Jr, et al.: Grimech 3.0 reaction mechanism, Sandia National Laboratory, 2000.
[23] F. Zhang, T. Zirwes, P. Habisreuther, H. Bockhorn: Effect of unsteady stretching on the flame local dynamics. Combust Flame 175, 170-179, 2017.
[24] T. Zirwes, F. Zhang, Y. Wang, P. Habisreuther, J.A. Denev, Z. Chen, H. Bockhorn, D. Trimis. In-situ flame particle tracking based on barycentric coordinates for studying local flame dynamics in pulsating Bunsen flames. Proc. Combust. Inst. 38(2), 2057-2066, 2021.